04.80.04 ·

Nuclear Engineering and Design 56 (1980) 83–89
North-Holland Publishing Company

THEORETICAL FUEL ELEMENT MODELLING AT CNEA *

S. HARRIAGUE, E.J. SAVINO, G. COROLI
Gerencia de Desarrollo, Comisión Nacional de Energía Atómica, Argentina

and

F.G. BASOMBRÍO and G. SÁNCHEZ SARMIENTO
Centro Atómico Bariloche, Comisión Nacional de Energía Atómica, Argentina

Received 17 March 1978

Computer codes and theoretical developments aiming to model nuclear reactor fuel elements at CNEA are reviewed. The codes PELT, VAINA and BACO for the overall fuel behaviour, as well as the finite element systems ELASTEF, PLASTEF and CTR are described. The influence on the BACO code predictions of including a fuel cracking model is discussed. Also, some examples of the calculated fuel cladding contact pressure are shown for different situations. Applications of the finite element systems to calculate the stress concentration at the skids of the Central Nuclear Atucha fuel rods and to predict local thermal effects of PuO_2 particles in a UO_2 fuel are discussed.

1. Introduction

In this paper we review the fuel element design and performance computer codes recently developed at CNEA.

Fuel element modelling demands that at least three lines of theoretical work are covered: (1) the development of codes for the overall fuel rod behaviour; (2) the development of codes for the description of localized phenomena in the fuel element; and (3) to tackle basic studies regarding materials behaviour under reactor operating conditions. This paper summarizes some of the achievements reached at CNEA along those lines. In section 2 a brief description is given of the computer codes being used at present. Section 3 gives some illustrative examples of application of those codes. In section 4 the main lines of theoretical work on materials behaviour under irradiation are presented, while section 5 gives some conclusions and future lines of work.

* This paper is a revised or up-dated version of the paper actually presented at the IAEA Specialists' Meeting on Fuel Element Performance Computer Modelling.

2. Computer codes in use

2.1. Overall behaviour codes

Three codes have been developed in order to cover the overall behaviour of the fuel element: PELT, VAINA and BACO. The basic philosophy behind the three codes is equivalent; they model, respectively, the state of stress and strain in a ceramic heat generating cylinder, in a metal cladding, and in a fuel rod section. The first two are used as new model testing codes, while the third is used as a fuel design and performance analysis code.

The assumptions of axial plane strain and axial symmetry allow the three-dimensional stress–strain problem to be reduced to a modified one-dimensional one. At present the following contributions to the state of stress and strain are considered: elastic distortion, thermal expansion, plastic deformation, creep, gas and solid products swelling, thermal and radiation induced redensification , axial and radial cracking, fuel reestructuring, and irradiation induced growth. The mechanical description is coupled with a self-consistent temperature calculation and a fuel gas release model.

The mathematical description of the mechanical

behaviour [1] is based on the assumption that the time variation of the strain in the principal direction (r, θ or z), for a finite but small time interval, can be expressed as a linear superposition of the individual strain variations due to the previously mentioned mechanisms under common stress and environmental conditions. Each of these strains can be written as an explicit function of the stresses at a given point. The mechanical state is described by those equations for the main strains plus the equilibrium and compatibility relations subject to the appropriate boundary conditions. In order to solve the numerical problem the axial section under study is divided into circular rings, and a finite difference scheme is applied. A central difference method is adopted; this should result in a relatively stable system of equations to be solved and it showed, when applied to the thermoelastic problem, better convergence than the forward difference scheme [2]. The nonlinear system of equations for the stresses in a time interval is linearized through a Taylor expansion. Whenever the tangential or axial stress at a given ring in the fuel exceeds a predefined fracture stress it is assumed that the ring is "cracked" in that direction. This implies that instead of solving the system of equations for the corresponding unknown main stress at the ring, this stress is considered as a known boundary condition and the system must be solved assuming an unknown crack strain η in that direction. If, during the time integration, η becomes negative, the crack is assumed to be closed or healed, depending on the temperature and stress at the ring.

The previously described system of linear equations for a given time increment can be solved for the main stresses by direct matrix inversion. A very efficient and fast numerical subroutine developed at Harwell [3] for inverting sparse matrixes is used. The finite difference method was chosen because of the following advantages as compared to analytical solutions: (i) the possibility of a simple treatment of cracks; (ii) the possibility of including the variation of material properties with temperature even if they are non linear; (iii) to be able to formulate the time dependence of the problem with explicit components; and (iv) the possibility of extending the calculation to include the interaction between fuel and cladding using the same numerical scheme.

One of the advantages of these codes is to have chosen the main stresses at each ring as the mathematical system unknowns. This allows the fuel–cladding contact to be solved without the need for cumbersome iterative procedures or ansatz for the contact pressure. When the contact is attained the boundary condition of radial stress on the fuel and cladding becomes unknown. This stress, i.e. minus the contact pressure, should satisfy, while the contact is maintained, the equality between the radial displacements at the internal cladding and the external fuel radii. The corresponding equation for this equality is then explicity added to the system. Whenever the contact pressure becomes negative, contact is assumed to be broken.

2.2. Localized phenomena codes

2.2.1 The ELASTEF system of codes for thermoelastic problems

The purpose of the ELASTEF [4] system of codes is to solve by the finite element method elastic and thermoelastic two-dimensional (plane stress or strain or axisymmetric stress) and nonhomogeneous problems of arbitrary geometric shape. Isolated points and/or portions of the boundary may be subject to:

(a) concentrated forces and/or distributed loads;
(b) imposed displacements;
(c) elastic boundary reactions; and
(d) any combination of the three previous boundary conditions.

Within those boundary conditions and under previously calculated spatial temperature distributions, the elastic displacements of the system are evaluated. From those displacements the strains, stresses and equivalent (von Mises) stresses are obtained at every point.

Triangular finite elements of uniform thickness are used for the calculation in cases of plane symmetry, and annular elements of triangular section for the axisymmetric ones. Linear interpolation is used within each element.

2.2.2. The PLASTEF codes for thermoelastoplastic problems

By using the finite element method these codes simulate the thermoelastoplastic behaviour of arbitrary-shaped structures [5,9]. For any strain hardening law and a given history of load and temperature, the deformation and stresses can be calculated by

using the hypothesis of plane stress, plane strain, or axisymmetric stress. The codes can deal both with a different strain hardening law and spontaneous discharges at any point of the structure during its load history.

The programs are based on the incremental initial-stress method. For each load and temperature increment a thermoelastic problem is solved with fictitious initial stresses and the results, which have been obtained from the equilibrium conditions, are stored. The problem is then solved by means of an iterative algorithm modifying the initial stresses. The iteration process is interrupted when the laws of plasticity are fulfilled within an acceptable error bound; the Levy–Prandtl–Reuss criterion of plasticity has been adopted. For each load increment the corresponding thermal strains are calculated with the temperature distribution obtained from the auxiliary code CUARM [6], and the thermoelastic incremental problem is solved with some of the routines of the ELASTIF system.

The program uses linear triangular elements. It has a total high speed memory requirement of about 100 kbytes, and it also needs auxiliary storage disks. This capacity allows triangular nets of about 300 elements and 200 nodes.

2.2.3. The CTR code for diffusion problems

This code [7] calculates a numerical solution of the transient quasi-harmonic equation in two independent spatial variables (plane or axial symmetry) within arbitrary-shaped ragions. Both nonhomogeneous Dirichlet and Neumann boundary conditions are allowed. The procedure is mathematically framed within the Galerkin–Faedo method. Linear triangular elements are used for the space integration, and a Crank–Nicholson finite differences scheme for the time. For a total high speed memory of 100 kbytes a problem involving a mesh of about 1100 elements and 800 nodes can be solved.

3. Examples of code applications

3.1. Influence of a cracking model on predicting the fuel performance

Some illustrative results of the BACO code have been given elsewhere [2,8]. In this section we discuss the influence of allowing for a fuel cracking model on predicting the behaviour of a fuel rod. This example will show the importance of the crack induced distortion on the other physical parameters predicted by the code and it will, at the same time, give an idea of the code's output and versatility.

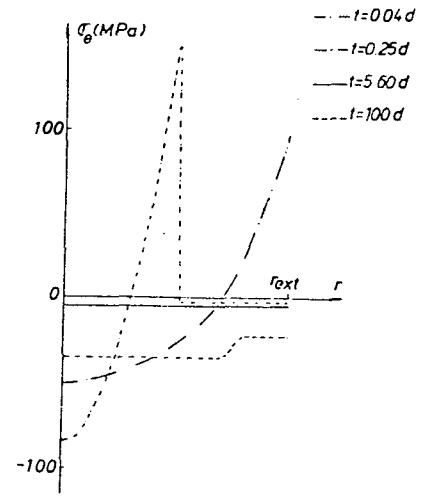

Fig. 1. Tangential stress as a function of the fuel radius for a CNA fuel at different times of a constant power cycle.

The code BACO was run for a section of a CNA (Central Nuclear Atucha) natural uranium fuel rod, assuming that it generates a constant linear power of 480 W/cm during 100 days and that this power has been reached in half a day linear increase. The fuel is assumed to be cracked at rings where a tangential or axial main stress of 150 MPa has been reached. The calculated central fuel temperature is 2090°C at the end of the power ramp and 1960°C at the end of the cycle. The tangential stress, calculated along the pellet radius, is plotted in fig. 1 at different times of the power cycle. * When a tangential or axial crack is open the corresponding main stress at the ring is assumed to be constant and equal to minus the gas pressure in the rod. It can be seen in fig. 1 that during the power rise the thermal fuel expansion creates a large tensile stress that is relaxed by tangential and axial cracks opening at the outer rings. The largest tensile main stress is then concentrated at the outermost uncracked ring – see $t = 0.25$ d, fig. 1. When a relatively large creep rate is attained at the tip of the crack (i.e. at constant power in this case) the stress at the pellet becomes compressive and the crack begins

* It must be remembered that the Atucha fuel is a solid cylindrical pellet.

to close. The closing down rate as well as the stress in the innermost rings show a large increment when fuel–cladding contact is reached; in this application the contact has occurred at 5.6 days. In the curves plotted in fig. 1 for 5.6 and 100 days of power it can be seen that the large amount of creep in the central region determines an almost hydrostatic state of stress.

In fig. 2 we compare the tangential stress at the end of the power ramp in the previously described case with an equivalent run where the pellet was not allowed to crack. We see that the cracking has relaxed the stresses by three orders of magnitude. Although for the case where the pellet is not allowed to crack the stress at the innermost rings is relaxed by creeping of the material, the allowance for cracking adds a large stress relaxation in the whole pellet. Also, the radial expansion of the pellet is larger by 11% if cracking is allowed; this difference implies in turn that the central temperature of the fuel is 84°C lower (2092°C against 2176°C) at that time. Since the uncracked fuel is hotter it emits more gases and the calculated gas

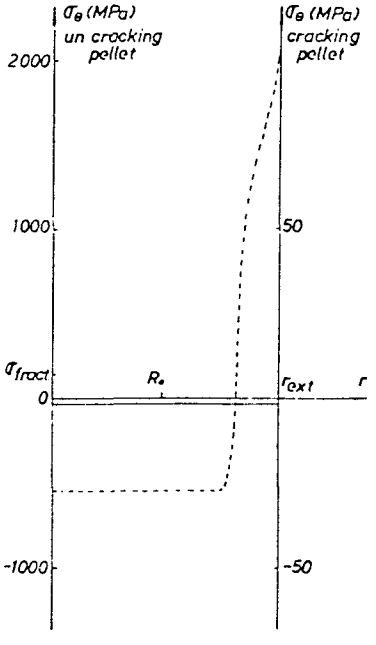

Fig. 2. Tangential stress at the end of the power ramp for a CNA fuel. The full curve corresponds to the fuel that was allowed to crack, and the dotted line denotes that cracking was not allowed. R_0 = crack penetration for the first case.

pressure during the power cycle is then larger in this case than in the case where the pellet is allowed to crack.

We conclude this example by amphasizing that the crack structure is strongly correlated with the stress-strain state of the material. This means that the results of the calculation where cracking is not allowed may not be extrapolated to give the behaviour of the cracked material. For example, in that case at the end of the power ramp the cracking stress of 150 MPa is reached at a radius of 0.82 r_{ext} – fig. 2 – while the tip of the crack is located at a radius $R_0 = 0.48\ r_{ext}$ if cracking is allowed for.

3.2. Contact pressure

In this example we show different applications of the unidimensional code, BACO, to cases where fuel–cladding contact is reached under different conditions. We especially emphasize the influence of the cladding creep law on the time needed for gap closure and the consequent stress increment at the cladding. In fig. 3(a) the power cycle to be simulated is sketched. This corresponds approximately to the cycle suffered by a CNA fuel element, where the fuel is transferred during operation from a low power peripheral channel at the reactor to a central position. The creep rate law proposed by Ross-Ross and Hunt (RR–H) [10] is used for the cladding. The law is modified in a second calculation by increasing the creep rate by a factor of 10 * and a third computer run is performed using the same cycle with no allowance for creep at the cladding. In fig. 3(b) the contact pressure calculated by the BACO code for the three cases is plotted. Owing to the creeping down of the cladding the pellet–cladding contact is reached much sooner in the case of the largest creep rate than in the other two, i.e. at 38.3 days against 96.7 and 101.7 for the RR–H creep and no creep cases, respectively. In the largest creep case the gap is then closed before the power rise; this determines a large increment in contact pressure at the ramp. However, the large value of the creep rate allows for a relatively

* This increment results in a creep rate of $1.3 \times 10^{-4}\ d^{-1}$ at $T = 367°C$, $\sigma = 50$ MPa, $\varphi = 7 \times 10^{13}$ n/(cm^{2}s)(characteristic values for the cladding) which is itself a sensible value if compared with other correlations [11].

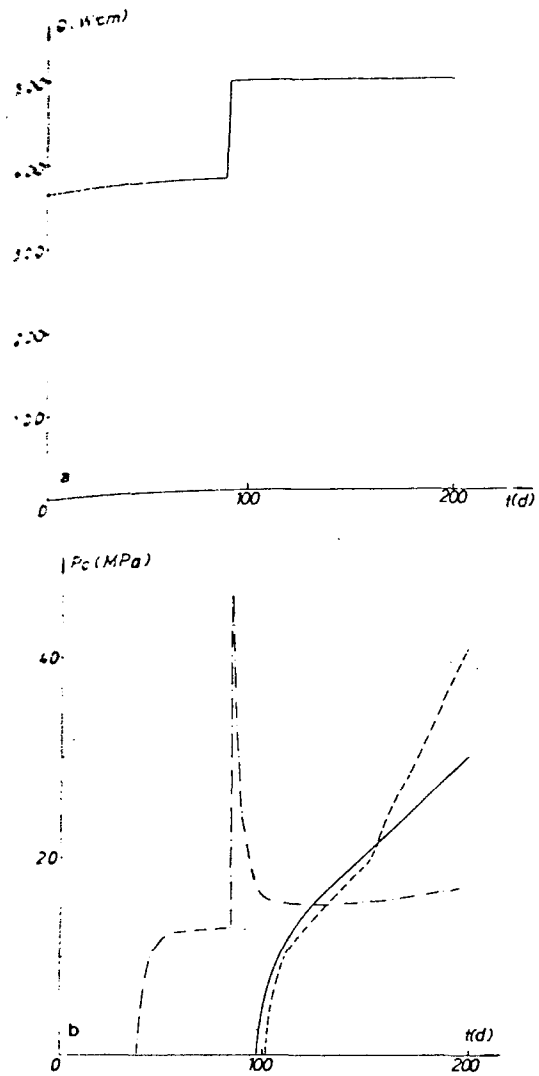

Fig. 3. (a) Power cycle used for simulation. (b) Calculated contact pressure for the cycle in (a) ——— using RR–H [10] creep rate law for the cladding; · – · – · RR–H creep rate law increased by an order of magnitude; - - - - - - no creep model included for the cladding.

quick stress relaxation when constant power is attained. After 200 days of full power the calculation using the largest creep rate predicts pressure values 43% smaller than those predicted by using the RR–H law, while the value calculated assuming no creep at the cladding is 35% larger.

3.3. Finite element thermoelastoplastic analysis of the Atucha fuel element cladding in the zone of the slider ribs

The clads of the CNA fuel rods have welded onto them a set of slider ribs of the same material, uniformly spaced among them. These ribs can slide longitudinally on the corresponding fuel element spacer so as to permit the free differential expansion (in the longitudinal direction) of the different rods that constitute the element. This cladding zone does not fulfil the hypothesis of the cylindrical infinite symmetry which is assumed in the unidimensional computer codes generally used to describe the overall thermomechanical behaviour of fuel rods. Therefore the final cladding resistance may differ in the neighbourhood of the ribs with respect to other sections of the rod.

In [9] a thermoelastoplastic bidimensional analysis corresponding to such a zone is described. The PLASTEF and the NOLICUARM codes were used for the resolution of the following limiting cases: (a) no initial cold gap between the ribs and the spacer, and (b) the initial gap is sufficiently larger as to remain open at any stage of the calculation, i.e. the presence of the spacer is ignored. In both limiting cases, for in-reactor conditions of temperature gradients and longitudinal stresses, the values of the thermoelastoplastic "collapse" pressure of the clad [9] were obtained (this internal pressure is due to the gases and to contact with the pellets). An elastoplastic law which includes strain hardening is used for simulating the cladding behaviour. In fig. 4 the advance of the plastic regions as

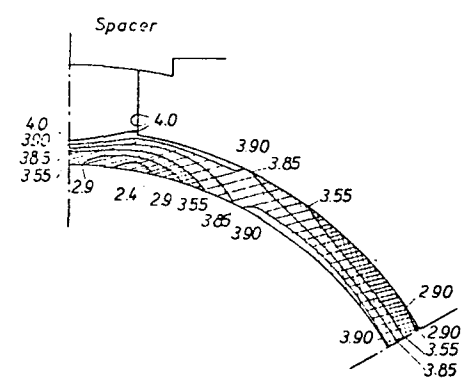

Fig. 4. Plastic zones close to the slider ribs of the CNA cladding for different values of the internal pressure p_i, in kg/mm^2.

a function of internal pressure for the previous described case (a) is plotted; the external pressure is taken equal to 1.2 kg/mm^2. A parallel analysis corresponding to the infinite clad without ribs was made, and the value obtained for the internal collapse pressure was almost identical to the previous ones. It is concluded that, with regard to the elastoplastic collapse, the ribs do not weaken the rod, contrary to what can be inferred from a purely thermoelastic calculation.

3.4. Evaluation of the local effects produced by particles of PuO_2 *in* UO_2 *fuel rods*

In a plutonium enriched UO_2 pellet, the PuO_2 should be in solid solution within the UO_2 matrix for a wide range of concentrations. However, if the solution is obtained by only a mechanical mixing of the oxides, PuO_2 islands are formed. These islands may be the source of several problems in the fuel behaviour, an important one being the overheating of the matrix in the neigbourhood of the particles. A detailed study of the thermal effects produced by PuO_2 particles in the UO_2 matrix must be performed in order to specify their permissible size. A section of the pellet with a distribution of PuO_2 particles was

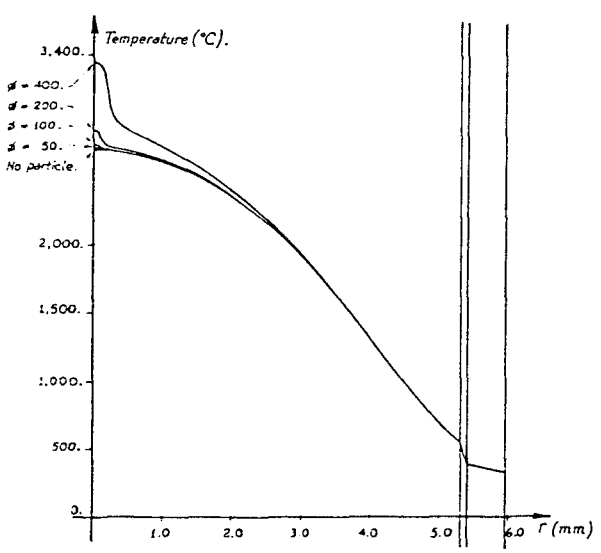

Fig. 5. Radial temperature distribution in a UO_2 fuel rod with a PuO_2 particle on its axis. The particle diameter ϕ (in μ) is taken as parameter.

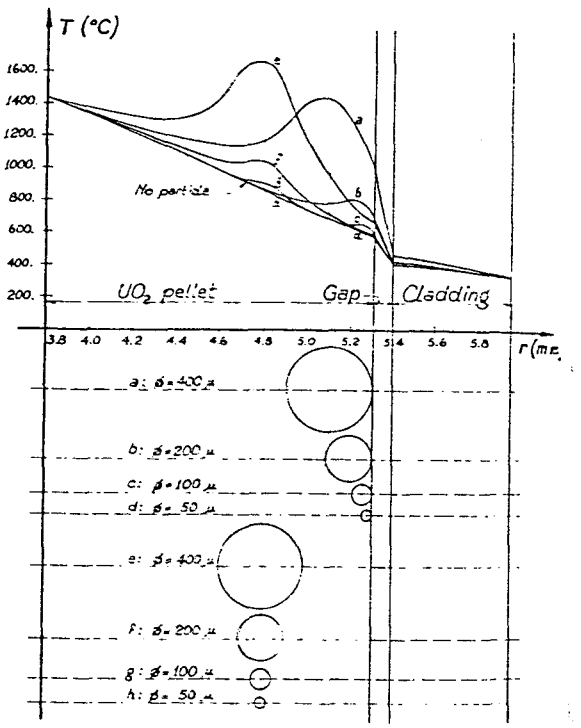

Fig. 6. Radial temperature distribution in a UO_2 fuel rod with a PuO_2 particle near the cladding. The particle diameter and position are indicated for each case.

studied. The spatial distribution of temperature and heat flux was calculated for a certain reactor power level as a function of the particles size [13]. The stationary nonlinear equation of heat conduction with temperature dependent conductivities has been solved by means of the finite element AXICUARM code [14]. The influence of PuO_2 islands on the temperature is shown in figs. 5 and 6 where the calculated radial temperature at a rod section is plotted for different island sizes and positions.

4. Basic theoretical work

In order to support and improve the mathematical description of the fuel behaviour under irradiation, a better understanding of the inherent material problems is imperative. Only this understanding can provide some confidence in the extrapolated behaviour which is necessarily far from laboratory conditions. The work in this area aims, for the time being, to understand

...clad properties under irradiation, with ... emphasis on the influence of the material ... on the mechanical behaviour under irradi... In this context theories of irradiation growth ... and creep [15,16] are being developed as well as ... work on simulation of intrinsic defects ... [17]. The radiation growth theory [14] ... for example, to correlate measured growth ... microstructural parameters (like loops and net... dislocation density) and the irradiation flux ... for a cold-worked zirconium alloy cladding ... structural core component.

Conclusions

The computer codes and some theoretical develop... tackled at CNEA in order to model and im... the understanding of the nuclear fuel perfor... under irradiation have been reviewed. Some ... examples are presented with the aim of ... the potentiality of the numerical meth...

The link between the three lines of work described ... is useful both to test the numerical ... among themselves and to provide a deeper ... of the fuel behaviour. In that connec... the predictions of the unidimensional codes are ... being compared with those provided by ... element method under equivalent load ... At the same time the unidimensional BACO ... being used for testing material models. The ... simple structure of the code and the large ... of physical phenomena included for the fuel ... allows, for example, to couple a complex rate theory of growth [14,16] with a whole fuel irradiation history [12] thereby providing an insight into the relation between microstructural parameters and fuel performance.

References

[1] S. Harriague, J.R. Matthews and E.J. Savino, Plan Multinacional de Metalurgia Report PMM/C222 (1977); AERE-M 2916 (1977).
[2] S. Harriague, C. Coroli and E.J. Savino, Nucl. Engrg. Des., to appear.
[3] Subroutine MA18 in AERE-R 7477 (1973).
[4] F.G. Basombrío, G. Sánchez Sarmiento and S. Pissanetzky, Report CNEA NT 28/78 (1978).
[5] F.G. Basombrío and G. Sánchez Sarmiento, Nucl. Eng. Des. 49 (1978) 231.
[6] F.G. Basombrío and B. Cruz, Report CNEA-NT 31/78 (1978).
[7] F.G. Basombrío and B. Cruz, Report CNEA-NT 30/78 (1978).
[8] S. Harriague, G. Coroli and E.J. Savino, 5th SMiRT Conf. (1979), Paper D1/2.
[9] F.G. Basombrío and G. Sánchez Sarmiento, Res. Mech. 1 (1979) (to be published).
[10] P.A. Ross-Ross and C.E.L. Hunt, J. Nucl. Mater. 26 (1968) 2.
[11] EPRI Report NP-369 (1977).
[12] E.J. Savino and S. Harriague, to be published.
[13] G. Sánchez Sarmiento, F.G. Basombrío and A. Marajofsky, Report CNEA NT 23/77 (1977).
[14] D. Fainstein-Pedraza, E.J. Savino and A. Pedraza, J. Nucl. Mater. 73 (1978) 151.
[15] E.J. Savino, Phil. Mag. 36 (1977) 323.
[16] E.J. Savino and C.E. Laciana, Int. Conf. on Fundamental Mechanisms of Radiation Induced Creep and Growth (1979).
[17] A.M. Monti, C.N. Tomé and E.J. Savino, Phys. Status Solidi (b) 92 (1979).